Poly-N-Acetylglucosamine Expression by Wild-Type Yersinia pestis Is Maximal at Mammalian, Not Flea, Temperatures

Poly-*N*-Acetylglucosamine Expression by Wild-Type *Yersinia pestis* Is Maximal at Mammalian, Not Flea, Temperatures

Pauline Yoong,* Colette Cywes-Bentley, and Gerald B. Pier

Channing Laboratory, Department of Medicine, Brigham and Women's Hospital, Harvard Medical School, Boston, Massachusetts, USA

* Present address: Department of Microbiology, New York University School of Medicine, New York, New York, USA.

ABSTRACT **Numerous bacteria, including *Yersinia pestis*, express the poly-*N*-acetylglucosamine (PNAG) surface carbohydrate, a major component of biofilms often associated with a specific appearance of colonies on Congo red agar. Biofilm formation and PNAG synthesis by *Y. pestis* have been reported to be maximal at 21 to 28°C or "flea temperatures," facilitating the regurgitation of *Y. pestis* into a mammalian host during feeding, but production is diminished at 37°C and thus presumed to be decreased during mammalian infection. Most studies of PNAG expression and biofilm formation by *Y. pestis* have used a low-virulence derivative of strain KIM, designated KIM6+, that lacks the pCD1 virulence plasmid, and an isogenic mutant without the pigmentation locus, which contains the hemin storage genes that encode PNAG biosynthetic proteins. Using confocal microscopy, fluorescence-activated cell sorter analysis and growth on Congo red agar, we confirmed prior findings regarding PNAG production with the KIM6+ strain. However, we found that fully virulent wild-type (WT) strains KIM and CO92 had maximal PNAG expression at 37°C, with lower PNAG production at 28°C both in broth medium and on Congo red agar plates. Notably, the typical dark colony morphology appearing on Congo red agar was maintained at 28°C, indicating that this phenotype is not associated with PNAG expression in WT *Y. pestis*. Extracts of WT sylvatic *Y. pestis* strains from the Russian Federation confirmed the maximal expression of PNAG at 37°C. PNAG production by WT *Y. pestis* is maximal at mammalian and not insect vector temperatures, suggesting that this factor may have a role during mammalian infection.**

IMPORTANCE ***Yersinia pestis* transitions from low-temperature residence and replication in insect vectors to higher-temperature replication in mammalian hosts. Prior findings based primarily on an avirulent derivative of WT (wild-type) KIM, named KIM6+, showed that biofilm formation associated with synthesis of poly-*N*-acetylglucosamine (PNAG) is maximal at 21 to 28°C and decreased at 37°C. Biofilm formation was purported to facilitate the transmission of *Y. pestis* from fleas to mammals while having little importance in mammalian infection. Here we found that for WT strains KIM and CO92, maximal PNAG production occurs at 37°C, indicating that temperature regulation of PNAG production in WT *Y. pestis* is not mimicked by strain KIM6+. Additionally, we found that Congo red binding does not always correlate with PNAG production, despite its widespread use as an indicator of biofilm production. Taken together, the findings show that a role for PNAG in WT *Y. pestis* infection should not be disregarded and warrants further study.**

Received 8 July 2012 **Accepted** 10 July 2012 **Published** 14 August 2012

Citation Yoong P, Cywes-Bentley C, Pier GB. 2012. Poly-*N*-acetylglucosamine expression by wild-type *Yersinia pestis* is maximal at mammalian, not flea, temperatures. mBio 3(4):e00217-12. doi:10.1128/mBio.00217-12.

Editor Liise-anne Pirofski, Albert Einstein College of Medicine

Address correspondence to Gerald B. Pier, gpier@channing.harvard.edu.

Enzootic transmission of *Yersinia pestis*, the etiologic agent of bubonic plague and pneumonic plague, involves passage between an infected mammalian host and a flea vector. It has been proposed that transmission is dependent on a biofilm formed by *Y. pestis* that physically blocks the proventriculus, the flea appendage needed for blood feeding (1), but other studies have shown that early transmission of bacteria by flea vectors does not involve biofilm formation (2). When a biofilm-based mode of transmission is involved, studies have indicated that blood feeding through the blocked proventriculus results in the ejection of *Y. pestis* directly into the bloodstream of the new host (3). Proteins encoded by the hemin storage (*hms*) operon are necessary for biofilm formation by *Y. pestis* (1). The genes of the *Y. pestis hms* operon are homologous to genes in the *pga* operon of *Escherichia coli* and the *ica* operon of *Staphylococcus aureus* and *S. epidermidis* (4, 5), both of which encode proteins required for the synthesis of the surface polysaccharide poly-*N*-acetylglucosamine (PNAG) (6, 7). *Y. pestis* appears to synthesize a PNAG-like surface polysaccharide, as antibodies raised to the polysaccharide component of the *S. epidermidis* biofilm, which comprises a β-1,6-GlcNAc polymer (the subunit present within PNAG molecules), reacted with *Y. pestis* biofilms, indicating that they are similar in structure (8, 9). In addition, dispersin B, a hexosaminidase from *Actinobacillus actinomycetemcomitans* that specifically hydrolyzes the glycosidic linkages of β-1,6-GlcNAc polymers, completely inhibits biofilm formation by *Y. pestis* (10) and *Y. pestis* biofilms were degraded by a β-hexosaminidase cloned from *Y. pseudotuberculosis* (9). The *Y. pestis* biofilm was bound by the lectins wheat germ agglutinin

and succinylated wheat germ agglutinin, both of which have binding specificity for β-GlcNAc moieties (11). Taken together, these findings strongly indicate that *Y. pestis* produces a surface polysaccharide composed of PNAG.

Thus far, the major pathogenic role of the *hms*-dependent biofilms formed by *Y. pestis* is in the colonization of the proventricular structure of fleas, a crucial step in the transmission of plague bacteria (1, 3). That conclusion was strengthened by the belief that the *Y. pestis* biofilm was maximally formed at a temperature of ~28°C but poorly or not at all at mammalian temperatures, i.e., ≥37°C (12). However, a review of the papers reporting this attribute of biofilm formation has revealed that this finding is based on results obtained with a single avirulent derivative of *Y. pestis* strain KIM, the *hms*$^+$ strain designated KIM6+ by Perry and coworkers, and an isogenic variant designated KIM6, which lacks the 102-kb *pgm* locus that contains the *hmsHFRS* operon and which is referred to here as KIM6 (Δ*pgm*) (2–4, 8, 12–16). KIM6+ was derived from wild-type (WT) strain KIM by deletion of the pCD1 virulence plasmid which contains the genes for the type III secretion proteins that are the major determinants of high-level virulence in plague bacteria. Erickson et al. (9) found that when they cloned a PNAG-degrading β-hexosaminidase from *Y. pseudotuberculosis* into KIM6+ *Y. pestis* there was reduced biofilm formation *in vitro* and a reduction in the proventricular blockage of fleas. However, microarray analysis of WT *Y. pestis* recovered from the lungs of infected mice showed that genes of the *hms* operon were upregulated during experimental pneumonic infection (17, 18), although its role in active infection has not been delineated. Lack of data on PNAG expression by WT *Y. pestis* and increased transcription of the *hms* genes during experimental mouse infection with WT strains suggested the possibility that WT *Y. pestis* does not show the same variation in PNAG production at 28 and 37°C as the KIM6+ derivative does. We thus investigated PNAG production among WT *Y. pestis* strains KIM and CO92 and sylvatic strains from the Russian Federation, where plague is endemic, to determine if they regulate polysaccharide synthesis in the same temperature-dependent manner as strain KIM6+.

RESULTS

Detection of PNAG by confocal microcopy and FACS analysis of WT and pCD1-negative strains of *Y. pestis* grown at 28 or 37°C. Using *Y. pestis* cells grown in brain heart infusion broth (BHIB), we confirmed results from prior publications (12, 13, 15, 16) showing the pCD1-negative KIM6+ strain of *Y. pestis* exhibited strong production of PNAG at 28°C, as evidenced by confocal immunofluorescence microscopy (Fig. 1A), which was markedly diminished at 37°C. The KIM6 (Δ*pgm*) strain, without the *pgm* locus, which also lacks the *hms* biosynthetic genes for PNAG, showed the same lack of reactivity with Alexa Fluor 488 (AF488)-conjugated monoclonal antibody (MAb) F598 to PNAG as it did with control MAb F429-AF488 specific to *P. aeruginosa* alginate (Fig. 1A). Treatment of KIM6+ cells grown in BHIB at 28°C with chitinase, which has no effect on PNAG, retained reactivity with MAb F598-AF488, whereas digestion with the PNAG-hydrolyzing enzyme dispersin B markedly diminished the reactivity of cells with MAb F598-AF488 (Fig. 1B).

In contrast to the data contained in numerous reports on the use of these two KIM6 variants (12, 13, 15, 16), we found that PNAG expression on cells of pCD1-positive WT *Y. pestis* KIM grown in BHIB at 37°C was greater than that on cells grown at

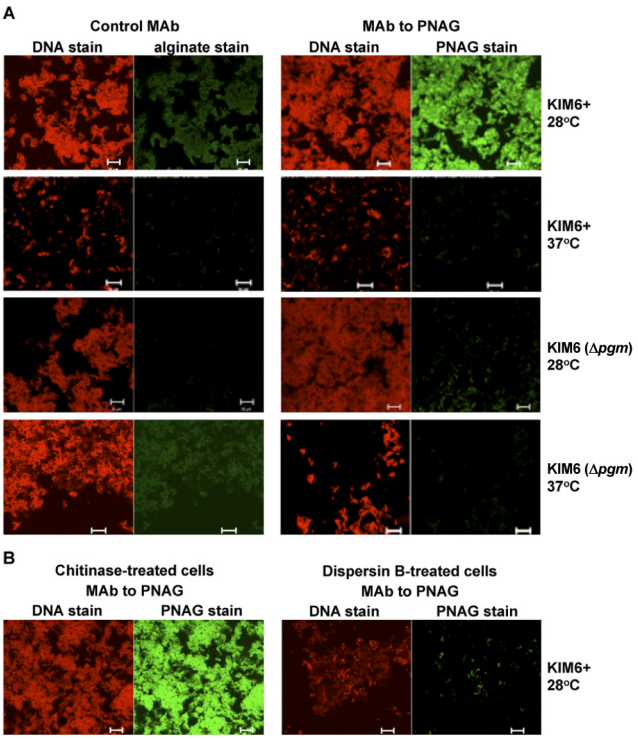

FIG 1 (A) Confocal microscopic analysis of PNAG expression by avirulent *Y. pestis* strain KIM6+ or KIM6 (Δ*pgm*) grown at either 28 or 37°C overnight in BHIB. (B) Reactivity of *Y. pestis* strain KIM6+ grown at 28°C with MAb F598-AF488 to PNAG after treatment of bacterial cells with either chitinase (control) or the PNAG-degrading enzyme dispersin B. Bars, 10 μm.

28°C (Fig. 2A). Similarly, WT *Y. pestis* CO92 cells showed little to no PNAG expression at 28°C in BHIB and marked expression at 37°C (Fig. 2A), which is the complete opposite of the results obtained over the past decades with the pCD1-negative derivatives of strain KIM (KIM6+). These outcomes were obtained with three separate samples of WT cells provided by the NERCE (New England Research Center for Excellence) Microbiology and Animal Core facility. WT *Y. pestis* KIM or CO92 cells grown in BHIB and treated with chitinase retained reactivity with MAb F598-AF488, whereas dispersin B treatment resulted in loss of immunoreactivity (Fig. 2B), indicative of PNAG production by WT *Y. pestis* cells.

Fluorescence-activated cell sorter (FACS) analysis of PNAG expression by the KIM pCD1-negative *Y. pestis* variants and WT strains KIM and CO92 following growth in BHIB correlated with the confocal immunofluorescence microscopy findings (Fig. 3A). For the pCD1-negative KIM6+ strain, FACS analysis showed higher levels of PNAG production when cells were grown at 28°C, with little made by cells grown at 37°C, while the *hms*-negative KIM6 strain had no reactivity above that of the control when grown at either 28 or 37°C (Fig. 3A, top). For WT strains KIM and CO92, FACS confirmed the higher expression of PNAG by cells grown at 37°C than by those grown at 28°C (Fig. 3A, bottom). Quantification of the mean fluorescence intensity obtained when comparing WT *Y. pestis* cells grown at either 28 or 37°C using MAb F598-AF488 to PNAG indicated that strain KIM produced about 2.6 times as much PNAG as with control MAb F498-AF488 at 28°C, while at 37°C, the expression of PNAG was increased to 14 times the background level and was comparable to that of the

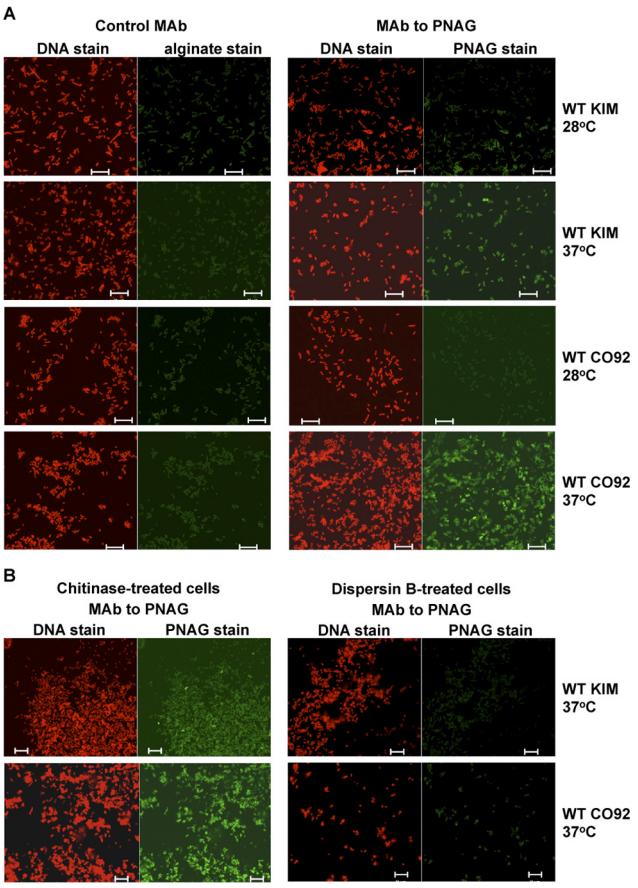

FIG 2 (A) Confocal microscopic analysis of PNAG expression by WT *Y. pestis* strain KIM or CO92 grown at either 28 or 37°C overnight in BHIB. (B) Reactivity of *Y. pestis* strain KIM or CO92 grown at 37°C with MAb F598-AF488 to PNAG after treatment of bacterial cells with either chitinase (control) or the PNAG-degrading enzyme dispersin B. Bars, 10 μm.

pCD1-negative KIM6+ strain grown at 28°C (Fig. 3B). For WT *Y. pestis* strain CO92, the FACS analysis also validated the confocal microscopic analysis in that only a small amount of PNAG was produced at 28°C (1.2 times the background level), while an increase to about 122 times the background level was seen when cells were grown at 37°C (Fig. 3B). Essentially identical results were obtained with three separate preparations of WT *Y. pestis* cells grown in BHIB.

Phenotypic appearance of *Y. pestis* colonies on Congo red agar. Growth of the pCD1-negative KIM6 (Δ*pgm*) and KIM6+ strains on Congo red agar resulted in the expected appearance of clear, light colonies of strain KIM6 (Δ*pgm*) at both 28 and 37°C (Fig. 4) and similar colonies of strain KIM6+ at 37°C, while dark-pigmented colonies were observed when this strain was grown at 28°C. For WT strains KIM and CO92, the dark-pigmented colonies were similarly seen when cells were grown at 28°C and not at 37°C (Fig. 4).

To determine if the dark-pigmented colonies of WT *Y. pestis* grown at 28°C on Congo red agar reflected a difference in PNAG production in this medium from that observed in BHIB, we analyzed the strains grown on Congo red agar by both confocal microscopy and FACS analysis for PNAG production. On Congo red agar, PNAG expression was very similar to that found in strains grown in broth: strain KIM6 (Δ*pgm*) expressed no detectable PNAG by either microcopy (Fig. 5) or FACS analysis (see Fig. 7); strain KIM6+ made PNAG at 28°C but not at 37°C (Fig. 5; see Fig. 7); WT strain KIM made PNAG at both temperatures (Fig. 6 and 7), with somewhat more detectable by FACS at 37°C (Fig. 7); and WT strain CO92 made much more PNAG at 37°C than at 28°C (Fig. 6 and 7). Thus, while the colony phenotype of Congo red agar for the pCD1-negative strains correlated with PNAG expression, this was not seen with the WT strains, indicating that the dark pigmentation seen on Congo red is not associated with the quantitative amounts of PNAG made by the cells in the culture.

PNAG production by *Y. pestis* isolates from the Russian Federation. Cell surface extracts immobilized on nylon membranes were prepared from diverse Russian sylvatic isolates of *Y. pestis* grown at 28 or 37°C. The strains were classified by biovar (19) and subspecies, with *Y. pestis* subsp. *pestis* representing the fully virulent form of *Y. pestis*. The results of immunoblot assays performed with an antiserum from a rabbit immunized with deacetylated PNAG (dPNAG) conjugated with diphtheria toxoid (DT) are summarized in Table 1. As expected, extracts from four *pgm*-negative, and hence *hms*-negative, strains of *Y. pestis* subsp. *pestis* did not bind the antibody to PNAG. Extracts from four *pgm*-positive *Y. pestis* subsp. *pestis* strains of two different biovars gave positive signals when cultures were grown at both 28 and 37°C, with higher expression at 37°C. Extracts from *Y. pestis* strain 1146, a *pgm*$^+$ *Y. pestis* biovar Antigua subsp. *caucasica* isolate, gave a positive signal when cultures were grown at 37°C but not when they were grown at 28°C, while extracts from another *Y. pestis* biovar Antigua subsp. *caucasica* isolate, P-1680, did not yield signals when cultures were grown at either temperature. Overall, the virulent *pgm*$^+$ *Y. pestis* subsp. *pestis* isolates produced PNAG in a manner analogous to that of WT strain KIM, which also originated in the same region of the world, whereas strain 1146 produced PNAG in a manner analogous to that of WT *Y. pestis* strain CO92, with little detected at 28°C and more detected at 37°C. None of these isolates behaved like the pCD1-negative KIM6+ strain, which showed greater PNAG production at 28°C than at 37°C.

DISCUSSION

The *hms* operon of *Y. pestis* strain KIM6+ is required for biofilm formation *in vitro* and the production of an aggregate of *Y. pestis* cells in the flea foregut (9), phenotypes linked to the transmission of this pathogen from this insect vector to a mammalian host (1, 3). The initial phenotype associated with the expression of the *hms* genes in *Y. pestis* was production of dark red colonies on Congo red agar plates (12), and this was later linked to PNAG production and biofilm formation (8, 9). Our findings do not dispute these previously published reports indicating that PNAG is synthesized maximally by *Y. pestis* KIM6+ at 28°C, as we also found higher PNAG production by this strain at 28°C, as determined by confocal microscopy and FACS analysis. However, it now appears that synthesis of PNAG by WT *Y. pestis* strains is not associated with the dark colony phenotype on Congo red agar, as we found that this phenotype occurred at 28°C in all of the *Y. pestis* stains tested, whereas PNAG production by WT strains was maximal at 37°C. Thus, the reported temperature regulation that links the maximal expression at 28°C of the phenotypes of dark red colonies on Congo red agar, PNAG production, and biofilm formation does not appear to occur in WT *Y. pestis*. Congo red is a somewhat

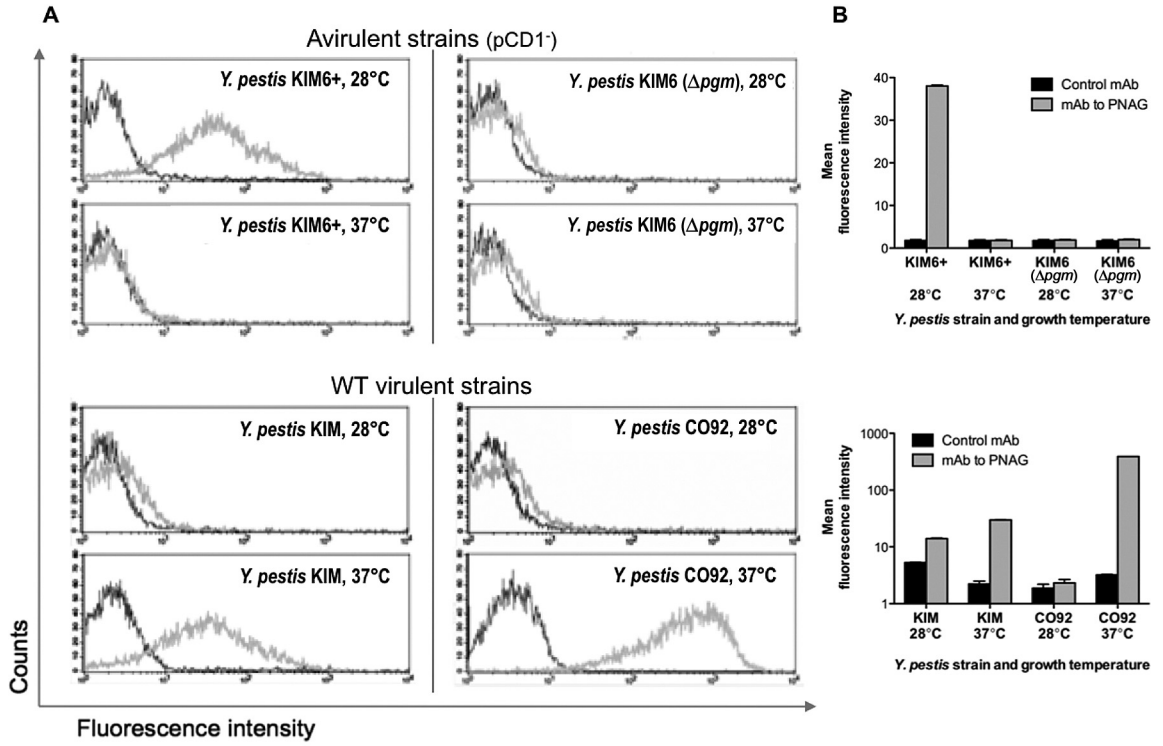

FIG 3 (A) Expression of PNAG by the indicated strains of *Y. pestis* grown in BHIB at the temperatures indicated in individual panels as determined by FACS. Dark gray trace, reactivity with control MAb F429 to *P. aeruginosa* alginate. Light gray trace, reactivity with PNAG-specific MAb F598. (B) Quantitative analysis of fluorescence intensity of *Y. pestis* strains reacted with either control MAb F429 (black bars) or MAb F598 to PNAG (gray bars). Bars indicate means, and error bars indicate the standard errors of the means.

nonspecific dye that has been shown to bind multiple polysaccharides (20), as well as proteins (21). Its reactivity with *Y. pestis* strains at lower temperatures suggests a possible interaction with a non-PNAG temperature-regulated molecule.

Given our findings that the KIM6+ strain does not regulate PNAG production as do WT *Y. pestis* strains (including the WT KIM strain from which KIM6+ was derived), PNAG production by KIM6+ may not be representative of what would occur in a comparison of WT *Y. pestis* with an isogenic Δ*hms* strain. It is likely that some genetic event occurred in the KIM6+ strain leading to the differential regulation of *hms* genes and/or Hms proteins that is not representative of WT *Y. pestis*. This could be attributed to the fluidity of the *Y. pestis* genome, which contains a large number of insertion sequences, predisposing it to chromosomal deletions and rearrangements (22, 23).

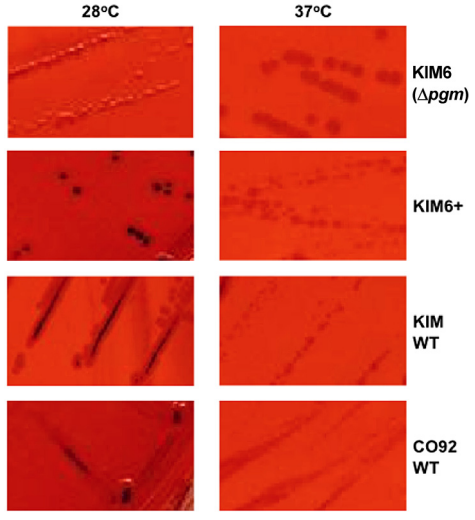

FIG 4 Colony morphology on Congo red agar of four *Y. pestis* strains grown overnight at the temperatures indicated. Only *pgm*/*hms*-positive strains produced dark-staining colonies at 28°C and not at 37°C.

In *Y. pestis*, biofilm formation and dispersion are largely regulated by two proteins, HmsT and HmsP (14). These proteins bridge the signal cascade between transmembrane sensors that detect environmental changes and downstream proteins involved in changing bacterial physiology in response to that signal, using cyclic di-GMP as the intermediate messenger (24, 25). HmsT is a diguanylate cyclase that synthesizes cyclic di-GMP, while HmsP is a phosphodiesterase that degrades cyclic di-GMP (26, 27). In KIM6+, several Hms proteins are posttranslationally regulated by protease degradation upon a temperature increase from 26 to 37°C (12, 14). Degradation of HmsT, the diguanylate cyclase that triggers biofilm formation at 37°C (in KIM6+) could explain the biofilm reduction seen at that temperature. While we have not attempted to pinpoint the differences between KIM6+ and WT *Y. pestis* strains that could have resulted in differential PNAG production, it seems plausible to hypothesize that differences or mutations in any protein(s) involved in the complex signal cascade could change the amount of PNAG synthesized in response to a temperature shift. Additionally, quorum sensing in *Y. pestis* is also

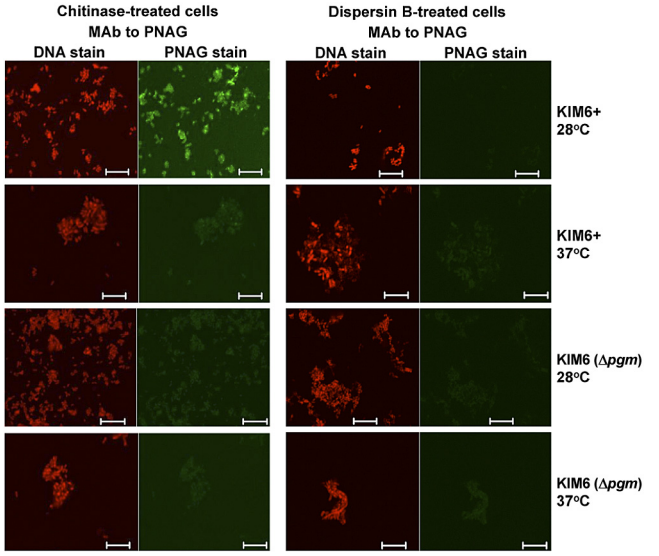

FIG 5 Confocal microscopic analysis of PNAG expression by avirulent *Y. pestis* strain KIM6+ or KIM6 (Δ*pgm*) grown at either 28 or 37°C overnight on Congo red agar. Reactivity with MAb F598-AF488 to PNAG after treatment of bacterial cells with either chitinase or the PNAG-degrading enzyme dispersin B. Bars, 10 μm. No binding of control MAb F429-AF488 was observed (not shown).

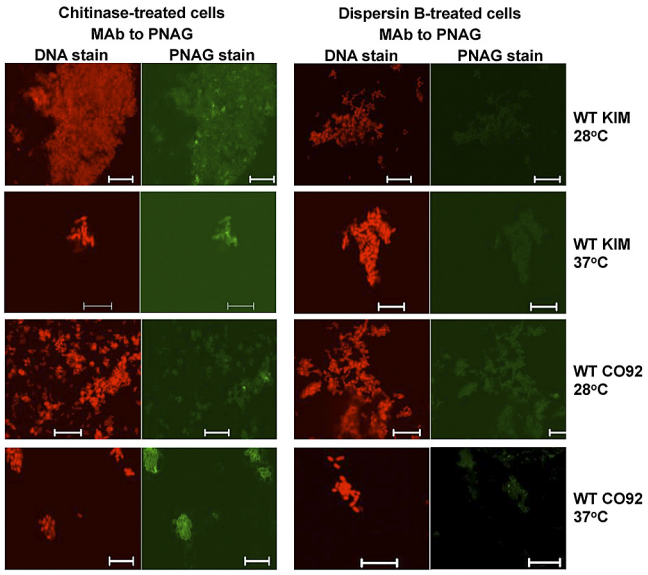

FIG 6 Confocal microscopic analysis of PNAG expression by WT *Y. pestis* strain KIM or CO92 grown at either 28 or 37°C overnight on Congo red agar. Reactivity with MAb F598-AF488 to PNAG after treatment of bacterial cells with either chitinase or the PNAG-degrading enzyme dispersin B. Bars, 10 μm. No binding of control MAb F429-AF488 was observed (not shown).

temperature regulated, with a change in the protein expression profile when a high cell density is reached (28). Proteins involved directly in, or upstream of, PNAG production may be regulated differently in KIM6+ in response to the achievement of quorum density, potentially also resulting in changes in biofilm formation.

Overall, we have confirmed that *Y. pestis* produces PNAG antigen but have also shown that the avirulent KIM6+ derivative does not regulate PNAG production as do WT *Y. pestis* strains. We believe that the prior general conclusion of increased PNAG production and biofilm formation at 21 to 28°C by *Y. pestis* (12, 13) was due to the sole use of the KIM6+ strain to determine these phenotypes, whereas maximal PNAG production by WT *Y. pestis* occurs at 37°C. However, despite the increased production of PNAG at mammalian temperatures by WT *Y. pestis*, any role it may have in virulence has yet to be elucidated. Unfortunately, conclusions regarding the lack of a role for PNAG in the virulence of *Y. pestis* are confounded by the use of KIM6+ restored to full virulence by the reintroduction of pCD1 (15, 26). Strains lacking *pgm* are attenuated, although the reduction in virulence has been attributed largely to the loss of an iron uptake protein (Irp2) found within the *pgm* pathogenicity island (29, 30). Notably, *pgm*$^+$ Δ*irp2* strains are still more virulent that Δ*pgm* strains, suggesting that other genes in the *pgm* genetic element play roles in infection and pathogenesis (31). In a study with a CO92 derivative, an inactivating mutation in *hmsP* (resulting in a strain deficient in biofilm breakdown) rendered the strain 100-fold more resistant than its parental strain to the antibiotic gentamicin (32). In the same study, an *hmsP* mutant was found to be deficient in the invasion of human lung fibroblast cells. Interestingly, Δ*hmsP* mutants were attenuated in mouse infection models, albeit these infections were established with KIM6+-derived strains (26). Taken together, these results suggest that while Hms proteins (and PNAG production) may be dispensable in the initial stage of infection, PNAG production could possibly confer an advantage on the bacteria once infection has been established. The finding that transcription of the *hms* genes by WT strain CO92 is increased during active pneumonic plague infection in a murine model (17, 18) would support the possibility that PNAG production and biofilm formation play a role later in infection, potentially protecting bacteria from antibiotics and host defenses. The fact that the KIM6+ derivative does not regulate PNAG production *in vivo* in the same way as WT *Y. pestis* does, coupled with the finding that PNAG production is maximal at 37°C *in vitro* and in a model of active plague infection, leaves opens the possibility that PNAG may have a role in *Y. pestis* virulence.

MATERIALS AND METHODS

Bacterial strains and growth conditions. *Y. pestis* WT strains KIM and CO92, along with strains KIM6+ (*pgm*$^+$ Hms$^+$) and KIM6 (Δ*pgm* Hms$^-$), kindly provided by Robert Perry, Louisville, KY, were used in these studies. All strains were verified as having the proper phenotype by the Microbiology and Animal Resources Core Laboratory of the NERCE in Biodefense and Emerging Infectious Diseases. For confocal microscopy and FACS analysis, all strains were grown at NERCE. A loopful of a frozen seed stock was streaked onto brain heart infusion agar and incubated for 2 days at 28°C. Next, several colonies were inoculated into 1 ml BHIB and mixed for 1 min and then 4 ml additional BHIB was added. The suspension was adjusted to an optical density at 650 nm of 1.0, and 1 ml thereof was inoculated into 50 ml of BHIB in a 250-ml vented, baffled flask and incubated at either 37 or 28°C with shaking at 200 rpm for 16 to 18 h. A similar procedure was used to grow colonies on Congo red agar plates for 48 h at either 28 or 37°C. The Congo red agar medium used (20 ml per plate) consisted of 37 g/liter of BHIB (Oxoid), 50 g/liter sucrose, 10 g/liter agar, and 400 mg/liter of sterile Congo red, which was added after sterilization by autoclaving, followed by cooling to 55°C.

After growth, cells were recovered by centrifugation, resuspended in 1 ml phosphate-buffered saline (PBS), and mixed thoroughly. Additional PBS was added (4 ml), and the cells were centrifuged again and resuspended in 1 ml of sterile 10% formalin. An additional 4 ml of 10% formalin was added, and the cultures were stored at 28°C for 4 days. Prior to the

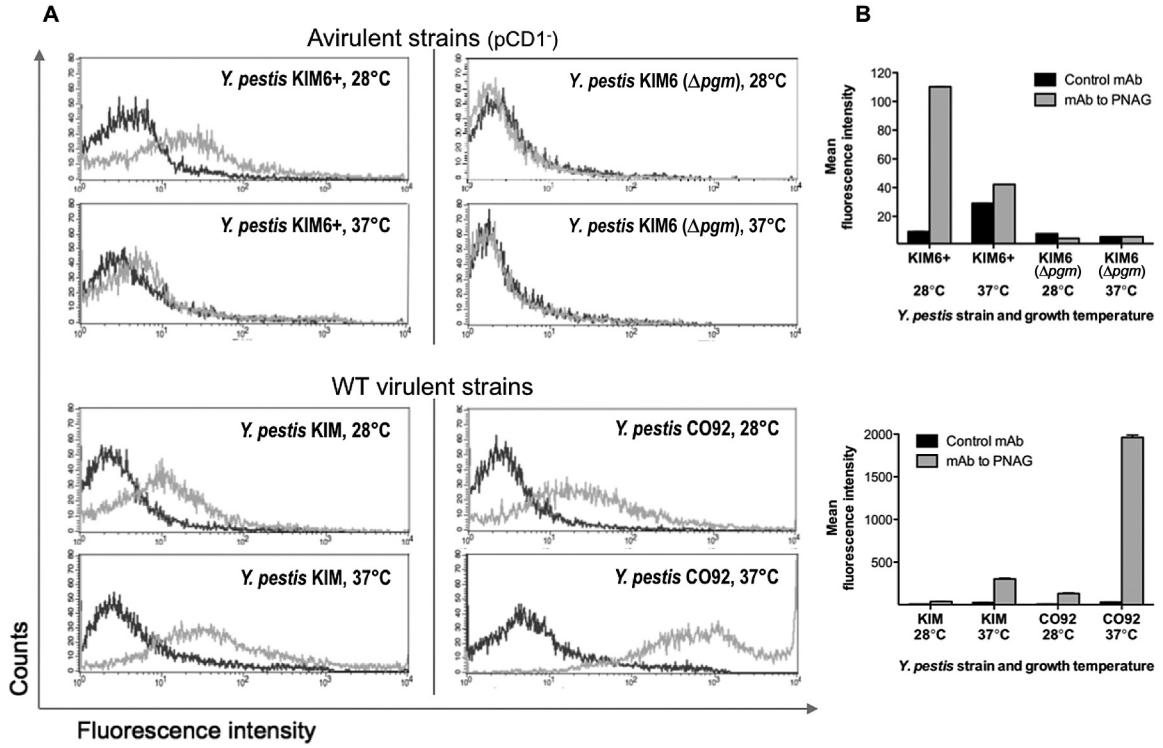

FIG 7 (A) Expression of PNAG by the indicated strains of *Y. pestis* grown on Congo red agar at the temperatures indicated in individual panels as determined by FACS analysis. Dark gray trace, reactivity with control MAb F429 to *P. aeruginosa* alginate. Light gray trace, reactivity with PNAG-specific MAb F598. (B) Quantitative analysis of fluorescence intensity of *Y. pestis* strains reacted with either control MAb F429 (black bars) or MAb F598 to PNAG (gray bars). Bars indicate means, and error bars indicate the standard errors of the means.

addition of formalin, an aliquot was taken to ascertain the number of CFU/ml by dilution and plating on blood agar plates (tryptic soy agar plates supplemented with 5% sheep blood). The colony counts of all cultures grown at 28 or 37°C were between 3×10^8 and 4×10^8 CFU/ml. The sterility of the formalin-treated cultures was ascertained by adding 100 μl of each culture to duplicate tubes of BHIB that were then incubated for 4 days at 37°C. No growth in any sample was seen after formalin fixation. Samples were adjusted to a concentration of 3×10^8 CFU/ml, aliquoted, and frozen at −80°C until used.

Antibody to PNAG. Fully human MAb F598, which binds to both native and deacetylated glycoforms of the *S. aureus* PNAG molecule, was used in this study (33). Immune serum from a rabbit immunized with dPNAG-DT (34) was used for detection of PNAG by immunoblotting.

Confocal microscopy. For confocal microscopic visualization of PNAG production by *Y. pestis*, a 100-μl frozen aliquot of formalin-fixed cells was defrosted and centrifuged to recover the bacterial cells, which were suspended in 20 μl of PBS and then air dried on microscope slides. Samples were fixed to the slides by exposure to 100% methanol for 1 min at room temperature, washed twice with PBS, and then labeled either with a control human IgG1 MAb, F429, specific to *P. aeruginosa* alginate (35) or with PNAG-specific human IgG1 MAb F598 (33), both of which were directly conjugated to AF488 (final MAb-fluorophore concentration,

TABLE 1 Summary of PNAG immunoblot assay results of cell surface extracts of diverse Russian laboratory or field isolates of *Y. pestis*

Strain	Biovar/subspecies	*pgm*	PNAG antibody binding[c] when grown at:	
			28°C	37°C
KIMD1	Medievalis/pestis	−	−	−
260(11)	Antigua/pestis	−	−	−
EV11M	Antigua/pestis	−	−	−
K1(780)[a]	Medievalis/pestis	−	−	−
KM239	Medievalis/pestis	+	+	++
625(44)[a]	Medievalis/pestis	+	+	++
260(5)	Antigua/pestis	+	+	++
U2357	Medievalis/altaica	+	+	++
P-1680[a,b]	Antigua/caucasica	+	−	−
1146[b]	Antigua/caucasica	+	−	+

[a] This strain carries the pCD1 virulence plasmid.
[b] This strain was not virulent in a guinea pig infection model.
[c] −, no binding; +, positive binding; ++, exceptionally strong binding.

5.2 μg/ml) along with the DNA-binding dye Syto 83 at 4 μM in PBS containing 0.5% bovine serum albumin (BSA). Staining reaction mixtures were incubated overnight at 4°C. Slides were washed twice with PBS and mounted for visualization by confocal microcopy.

To verify that the material reacting with PNAG-specific MAb F598 was likely PNAG, additional formalin-fixed samples were washed and resuspended in 200 μl of Tris-buffered saline (pH 6.8) containing either 50 μg/ml of the PNAG-hydrolyzing enzyme dispersin B (36) (Kane Biotech, Manitoba, Canada) or the chitin-degrading enzyme chitinase (Sigma), which has no effect on PNAG, and incubated overnight at 37°C. Cells were washed and reacted with MAb F598-AF488 as described above. Retention of MAb F598-AF488 binding following digestion with chitinase with loss of binding following digestion with dispersin B is indicative that the target antigen is PNAG.

FACS analysis. Frozen aliquots of formalin-fixed samples of *Y. pestis* cells were thawed and vortexed, and 300 μl of each sample was used to recover cells by centrifugation. The cells were washed with PBS with 0.5% BSA and split into three 100-μl aliquots. Samples were incubated overnight at 4°C with either 100 μl of PBS-BSA (unlabeled, used for calibration) or 5.2 μg/ml of either MAb F429 or MAb F598 directly conjugated with AF488. Samples were washed twice with PBS and resuspended in 500 μl of PBS before filtering through filter-cap FACS tubes and analyzed on a BD FACScalibur.

Immunoblot assays. Cell surface extracts obtained from *Y. pestis* strains from regions of the Russian Federation where plague is endemic in rodents (19) were subjected to treatment with proteinase K at 65°C for 5 h, followed by proteinase inactivation at 80°C for 30 min, and then spotted onto a nylon membrane that was provided to us by Andre Anisimov and colleagues at the State Research Center for Applied Microbiology and Biotechnology, Obolensk, Moscow Region, Russian Federation. The membrane containing the bacterial cell surface extracts was incubated with antisera from rabbits immunized with dPNAG conjugated with DT as the primary antibody at a 1:1,000 dilution, followed by horseradish peroxidase (HRP)-conjugated anti-rabbit IgG secondary antibodies that were used at a dilution of 1:10,000. Visualization was with substrate for the HRP enzyme.

ACKNOWLEDGMENTS

This work was supported by National Institutes of Health National Institute of Allergy and Infectious Diseases grants AI46706 and AI057159, a component of award no. U54 AI057159. The content of this report is solely our responsibility and does not necessarily represent the official views of the National Institute of Allergy and Infectious Diseases or the National Institutes of Health.

We thank Christine Anderson, Sean Fitzgerald, and colleagues at NERCE for preparation of WT *Y. pestis* cells; Andre Anisimov and colleagues from the State Research Center for Applied Microbiology and Biotechnology, Obolensk, Moscow Region, Russian Federation, for membranes with surface extracts from Russian plague bacterial strains; Robert Perry from the University of Kentucky for the *Y. pestis* strains used in this study; and Tomas Maira-Litran from the Channing Laboratory for producing the polyclonal antibody to PNAG.

G.B.P. is an inventor of intellectual property (IP; PNAG vaccine and MAb to PNAG) that is licensed by Brigham and Women's Hospital (BWH) to Alopexx vaccines LLC and Alopexx Pharmaceuticals LLC, companies in which G.B.P. owns equity. As an inventor of the IP, he also has the right to receive a share of licensing-related income (royalties, fees) through BWH from Alopexx Pharmaceuticals and Alopexx vaccines. G.B.P.'s interests were reviewed and are managed by BWH and Partners HealthCare in accordance with their conflict-of-interest policies.

REFERENCES

1. **Jarrett CO, et al.** 2004. Transmission of *Yersinia pestis* from an infectious biofilm in the flea vector. J. Infect. Dis. **190**:783–792.
2. **Vetter SM, et al.** 2010. Biofilm formation is not required for early-phase transmission of *Yersinia pestis*. Microbiology **156**:2216–2225.
3. **Hinnebusch BJ, Perry RD, Schwan TG.** 1996. Role of the *Yersinia pestis* hemin storage (hms) locus in the transmission of plague by fleas. Science **273**:367–370.
4. **Jones HA, Lillard JW, Jr, Perry RD.** 1999. HmsT, a protein essential for essential of the haemin storage (Hms+) phenotype of *Yersinia pestis*. Microbiology **145**:2117–2128.
5. **Wang X, Preston JF III, Romeo T.** 2004. The *pgaABCD* locus of *Escherichia coli* promotes the synthesis of a polysaccharide adhesin required for biofilm formation. J. Bacteriol. **186**:2724–2734.
6. **Cerca N, et al.** 2007. Molecular basis for preferential protective efficacy of antibodies directed to the poorly acetylated form of staphylococcal poly-*N*-acetyl-{beta}-(1-6)-glucosamine. Infect. Immun. **75**:3406–3413.
7. **Maira-Litrán T, et al.** 2002. Immunochemical properties of the staphylococcal poly-*N*-acetylglucosamine surface polysaccharide. Infect. Immun. **70**:4433–4440.
8. **Bobrov AG, Kirillina O, Forman S, Mack D, Perry RD.** 2008. Insights into *Yersinia pestis* biofilm development: topology and co-interaction of Hms inner membrane proteins involved in exopolysaccharide production. Environ. Microbiol. **10**:1419–1432.
9. **Erickson DL, Jarrett CO, Callison JA, Fischer ER, Hinnebusch BJ.** 2008. Loss of a biofilm-inhibiting glycosyl hydrolase during the emergence of *Yersinia pestis*. J. Bacteriol. **190**:8163–8170.
10. **Itoh Y, Wang X, Hinnebusch BJ, Preston JF III, Romeo T.** 2005. Depolymerization of β-1,6-*N*-acetyl-d-glucosamine disrupts the integrity of diverse bacterial biofilms. J. Bacteriol. **187**:382–387.
11. **Tan L, Darby C.** 2004. A movable surface: formation of *Yersinia* sp. biofilms on motile *Caenorhabditis elegans*. J. Bacteriol. **186**:5087–5092.
12. **Perry RD, et al.** 2004. Temperature regulation of the hemin storage (Hms^+) phenotype of *Yersinia pestis* is posttranscriptional. J. Bacteriol. **186**:1638–1647.
13. **Bobrov AG, Kirillina O, Perry RD.** 2007. Regulation of biofilm formation in *Yersinia pestis*. Adv. Exp. Med. Biol. **603**:201–210.
14. **Kirillina O, Fetherston JD, Bobrov AG, Abney J, Perry RD.** 2004. HmsP, a putative phosphodiesterase, and HmsT, a putative diguanylate cyclase, control Hms-dependent biofilm formation in *Yersinia pestis*. Mol. Microbiol. **54**:75–88.
15. **Lillard JWJ, Bearden SW, Fetherston JD, Perry RD.** 1999. The haemin storage (Hms+) phenotype of *Yersinia pestis* is not essential for the pathogenesis of bubonic plague in mammals. Microbiology **145**:197–209.
16. **Perry RD, Fetherston JD.** 1997. *Yersinia pestis*—etiologic agent of plague. Clin. Microbiol. Rev. **10**:35–66.
17. **Lathem WW, Crosby SD, Miller VL, Goldman WE.** 2005. Progression of primary pneumonic plague: a mouse model of infection, pathology, and bacterial transcriptional activity. Proc. Natl. Acad. Sci. USA **102**:17786–17791.
18. **Liu H, et al.** 2009. Transcriptional profiling of a mice plague model: insights into interaction between *Yersinia pestis* and its host. J. Basic Microbiol. **49**:92–99.
19. **Anisimov AP, Lindler LE, Pier GB.** 2004. Intraspecific diversity of *Yersinia pestis*. Clin. Microbiol. Rev. **17**:434–464.
20. **Teather RM, Wood PJ.** 1982. Use of Congo red-polysaccharide interactions in enumeration and characterization of cellulolytic bacteria from the bovine rumen. Appl. Environ. Microbiol. **43**:777–780.
21. **Khurana R, Uversky VN, Nielsen L, Fink AL.** 2001. Is Congo red an amyloid-specific dye? J. Biol. Chem. **276**:22715–22721.
22. **Buchrieser C, et al.** 1999. The 102-kilobase *pgm* locus of *Yersinia pestis*: sequence analysis and comparison of selected regions among different *Yersinia pestis* and *Yersinia pseudotuberculosis* strains. Infect. Immun. **67**:4851–4861.
23. **Parkhill J, et al.** 2001. Genome sequence of *Yersinia pestis*, the causative agent of plague. Nature **413**:523–527.
24. **Ryan RP, Fouhy Y, Lucey JF, Dow JM.** 2006. Cyclic di-GMP signaling in bacteria: recent advances and new puzzles. J. Bacteriol. **188**:8327–8334.
25. **Sondermann H, Shikuma NJ, Yildiz FH.** 2012. You've come a long way: c-di-GMP signaling. Curr. Opin. Microbiol. **15**:140–146.
26. **Bobrov AG, et al.** 2011. Systematic analysis of cyclic di-GMP signalling enzymes and their role in biofilm formation and virulence in *Yersinia pestis*. Mol. Microbiol. **79**:533–551.
27. **Bobrov AG, Kirillina O, Perry RD.** 2005. The phosphodiesterase activity of the HmsP EAL domain is required for negative regulation of biofilm formation in *Yersinia pestis*. FEMS Microbiol. Lett. **247**:123–130.
28. **Bobrov AG, et al.** 2007. Functional quorum sensing systems affect biofilm

formation and protein expression in *Yersinia pestis*. Adv. Exp. Med. Biol. **603**:178–191.
29. **Iteman I, et al.** 1993. Relationship between loss of pigmentation and deletion of the chromosomal iron-regulated *irp2* gene in *Yersinia pestis*: evidence for separate but related events. Infect. Immun. **61**:2717–2722.
30. **Sebbane F, Jarrett C, Gardner D, Long D, Hinnebusch BJ.** 2010. Role of the *Yersinia pestis* yersiniabactin iron acquisition system in the incidence of flea-borne plague. PLoS One **5**:e14379.
31. **Fetherston JD, Kirillina O, Bobrov AG, Paulley JT, Perry RD.** 2010. The yersiniabactin transport system is critical for the pathogenesis of bubonic and pneumonic plague. Infect. Immun. **78**:2045–2052.
32. **Leigh SA, Forman S, Perry RD, Straley SC.** 2005. Unexpected results from the application of signature-tagged mutagenesis to identify *Yersinia pestis* genes required for adherence and invasion. Microb. Pathog. **38**: 259–266.
33. **Kelly-Quintos C, Cavacini LA, Posner MR, Goldmann D, Pier GB.** 2006. Characterization of the opsonic and protective activity against *Staphylococcus aureus* of fully human monoclonal antibodies specific for the bacterial surface polysaccharide poly-*N*-acetylglucosamine. Infect. Immun. **74**:2742–2750.
34. **Maira-Litrán T, Kropec A, Goldmann DA, Pier GB.** 2005. Comparative opsonic and protective activities of *Staphylococcus aureus* conjugate vaccines containing native or deacetylated staphylococcal poly-*N*-acetyl-β-(1-6)-glucosamine. Infect. Immun. **73**:6752–6762.
35. **Pier GB, et al.** 2004. Human monoclonal antibodies to *Pseudomonas aeruginosa* alginate that protect against infection by both mucoid and nonmucoid strains. J. Immunol. **173**:5671–5678.
36. **Manuel SG, et al.** 2007. Role of active-site residues of dispersin B, a biofilm-releasing beta-hexosaminidase from a periodontal pathogen, in substrate hydrolysis. FEBS J **274**:5987–5999.